

Article

Evaluation of Bond Properties of a Fabric-Reinforced Cementitious Matrix for Strengthening of Concrete Structures

Min-Jun Kim ¹, Hyeong-Gook Kim ², Yong-Jun Lee ³, Dong-Hwan Kim ², Min-Su Jo ⁴
and Kil-Hee Kim ^{2,*}

¹ Land and Housing Institute, Korea Land and Housing Corporation, Daejeon 34047, Korea; minjunk@lh.or.kr

² Department of Architectural Engineering, Kongju National University, Cheonan 31080, Korea; anthk1333@kongju.ac.kr (H.-G.K.); kimdh@kongju.ac.kr (D.-H.K.)

³ Korea Construction Standards Center, Korea Institute of Civil Engineering and Building Technology, Goyang 10223, Korea; leeyj@kict.re.kr

⁴ CareCon Co., Ltd., Seoul 05586, Korea; jjangkku@naver.com

* Correspondence: kimkh@kongju.ac.kr; Tel.: +82-41-521-9335

Received: 23 April 2020; Accepted: 26 May 2020; Published: 29 May 2020



Abstract: In the present study, pull-out and pull-off tests were conducted to examine the bond strength between an inorganic cement adhesive (hereinafter referred to as the “matrix”) and a textile, which composed a fabric-reinforced cementitious matrix (FRCM). The matrix was developed by mixing slag and short fibers in an attempt to improve the alkali resistance and compressive strength. The developed matrix was examined with regard to its alkali resistance, water resistance, and void distribution. Bond tests were conducted in two parts: a pull-out series and pull-off series. The type of textile (carbon or basalt) and the weaving methods were selected as test parameters. These tests were performed in accordance with the methods described in ISO10406-1 (pull-out) and ASTM C1583 (pull-off). The test results showed that the developed matrix was superior to existing mortar methods in terms of alkali resistance, water resistance, and compressive strength. Additionally, the FRCM in which carbon textiles were used exhibited excellent bond performance.

Keywords: FRCM; cement-based matrix; textile reinforcement; pull-out; pull-off

1. Introduction

Reinforced concrete (RC) structures are subject to degradation of their structural stability as they are exposed to external loads such as earthquakes and to stress over time. Notably, cracks that occur on the concrete surfaces of RC structures negatively affect their serviceability and induce the corrosion of reinforcing bars, thereby resulting in the deterioration of structural performance. Thus, the safe use of RC structures requires effective repair and reinforcement methods that can control the cracking of concrete. Currently, steel plate reinforcement is mainly used for the repair and reinforcement of RC structures [1,2]. However, this method may be involved in problems related to reduced adhesive strength at the steel–concrete composite interface, as well as increased self-weight of structures. To overcome these problems, research has been actively carried out since the 1990s on fiber-reinforced polymer (FRP) reinforcement methods, where fiber sheets with a high tensile strength and elastic modulus are used [3–8].

The FRP reinforcement method is better than existing steel plate reinforcement when used for the repair and reinforcement of RC structures because it is lightweight, corrosion-resistant, and non-conductive. However, the FRP reinforcement method may cause fiber sheets to be detached from the concrete surface because the adhesive strength of the epoxy adhesive starts to decrease at

a temperature equal to or higher than a specific value (glass transition temperature). The method also has a disadvantage in that it cannot be applied to wet surfaces or at low temperatures. Furthermore, the low economic feasibility and toxicity of epoxy adhesive limit its serviceability [9].

To overcome these disadvantages of FRP reinforcement methods, research is now being conducted on reinforcement using fabric-reinforced cementitious matrix (FRCM). FRCM is a method where a cementitious matrix and textile are combined to reinforce the concrete surface [10]. In general, the cementitious matrix is a binder composed of Portland cement, silica fume, and fly ash. Carbon and glass fibers are widely used as textiles.

The FRCM reinforcement method provides improved economic feasibility and utility when compared to FRP reinforcement because the cementitious matrix is used instead of an epoxy bond. Additionally, the method may allow for high tensile strength and pseudo-ductile behavior depending on the type of used textile, and high durability is ensured because corrosion does not occur due to the intrinsic characteristics of the textiles [11]. These advantages have made FRCM reinforcement widely available for the repair and reinforcement of buildings and structures. However, when a matrix that composes the FRCM is highly alkaline, the durability of the used textiles may deteriorate. Thus, more research regarding this issue is needed [12,13].

Previous studies have conducted research on the bond between the matrix and textiles in attempts to examine the bond strength with respect to the properties of the matrix [14,15]. Additionally, many studies have performed bond tests, where the matrix and textiles were selected as test parameters and the strain behavior of textiles was examined with respect to the bond stress [16–26]. However, in previous studies, investigations into the alkalinity of the matrix, which may deteriorate the durability of textiles used in FRCM, have not been conducted. Recently, Colombo et al. [27], Portal et al. [28], and De Munck et al. [29] studied the durability of textiles but did not evaluate the durability of textiles applied to the FRCM.

In order to ensure the durability of the FRCM and effective reinforcement of RC elements, it is necessary to develop a matrix that is alkali-resistant [30,31]. Therefore, in the present study, a matrix with alkali resistance was developed in an attempt to achieve the required durability for the textiles used in the FRCM. Furthermore, to make the developed matrix available for the repair and reinforcement of RC elements, pull-out and pull-off tests were conducted as preliminary research. Based on these results, the bond characteristics between the developed matrix and the textile were evaluated.

2. Matrix

2.1. Mix Proportion of the Matrix

In the present study, a matrix with alkali resistance was developed to increase the bond strength of textiles. As shown in Table 1, the mix proportion of the matrix was formulated with the following factors as parameters to satisfy the required workability, adhesion with textiles, and durability: the amount of binder added, mix ratio of short fibers, and type and amount of polymer added. With this mix proportion considered, the target compressive strength and flexural strength were set to 60 and 16 MPa, respectively. As shown in Table 2, compressive and flexural strength tests were conducted according to the ISO 679: 2009 at the ages of 7 days and 28 days [32]. The obtained compressive strength and flexural strengths were 68.3 and 16.3 MPa, respectively.

Table 1. Mix properties (unit weight (g)).

Mix	Cement	Binder	Water	Short Fiber (PVA, 3 mm)	Polymer (EVA)	Sand	E.A	Superplasticizer
Matrix		840	340	4.0	4.0	1108.2	80.0	3.8
Mortar	700	-	320	-	-	1227	70.0	3.0

Cement: Ordinary Portland cement (Type I); Binder: Ordinary Portland cement + slag + silica fume; PVA: Polyvinyl alcohol 0.2%; EVA: Ethylene vinyl acetate 0.2%; Superplasticizer: Melamine F10, E.A: Expansive additive.

Table 2. Test results for the matrix.

Slump Flow (mm)	Compressive Strength (MPa)			Flexural Strength (MPa)		
	3 days	7 days	28 days	3 days	7 days	28 days
180	20.5	41.6	68.3	5.2	9.9	16.3

2.2. Evaluation of Alkali Resistance of the Matrix

In the present study, Alkali resistance test specimens were fabricated in accordance with KS F 4042 [33] to evaluate the durability of the matrix constituting the FRCM. As shown in Figure 1, alkali-resistant test specimens made from the developed matrix were immersed in a saturated calcium hydroxide solution at 50 ± 2 °C for 28 days. The durability of the developed matrix was compared with the existing mortar repair methods, as shown in Table 3. Meanwhile, the alkali resistance was also compared between the developed matrix and the existing mortar repair methods. The results showed that the degradation of compressive strength and flexural strength was about 70% and about 40% lower, respectively, in the developed matrix than in the existing mortar repair methods, as shown in Table 3.



Figure 1. Evaluation of alkali resistance of the matrix: (a) dipping; (b) curing (thermo-humidistat).

Table 3. Alkali resistance results.

Mix	Compressive Strength (MPa)			Flexural Strength (MPa)		
	Non-Immersion	Immersion *	Deterioration	Non-Immersion	Immersion *	Deterioration
Matrix	68.3	65.9	3.5%	16.3	15.3	6.1%
Mortar	61.7	54.8	11.0%	13.4	12.0	10.4%

* Calcium hydroxide solution.

2.3. Evaluation of the Water Resistance of the Matrix

Test specimens were fabricated to evaluate the water resistance of the developed matrix, as shown in Figure 2. The water resistance was measured according to the ASTM C1403: 15 with respect to the time duration, ranging from 0 to 1440 min, as shown in Table 4 [34]. The water resistance of the matrix developed in the present study was compared with that of the existing mortar repair methods. The results showed that water absorption was about 30% less on average in the developed matrix than in the existing mortar repair methods. It was confirmed that the developed matrix and the existing mortar methods had comparable water absorption coefficients of 0.10 and 0.11, respectively.

Table 4. Water resistance results.

Amount of Water Absorption (kg/m ²)	Time (min)					
	0	10	30	60	360	1440
Mortar	0	0.52	0.64	0.70	0.86	1.00
Matrix	0	0.31	0.39	0.43	0.62	0.82



Figure 2. Evaluation of the water resistance of the matrix: (a) specimens; (b) dipping.

2.4. Evaluation of Void Distribution of the Matrix

In general, the amount of air and the void structure of the matrix affect the compressive strength and freeze–thaw resistance. Thus, in the present study, the void distribution of the matrix while being hardened was analyzed, as shown in Figure 3. The void distribution of the matrix was measured using test specimens fabricated in accordance with ASTM C 457 [35]. The results were compared with those for the existing mortar repair method. It was found that the proportion of voids measuring less than 1 mm was lower in the developed matrix than in the mortar repair method. This observation confirmed that the developed matrix had better compressive strength and freeze–thaw resistance.

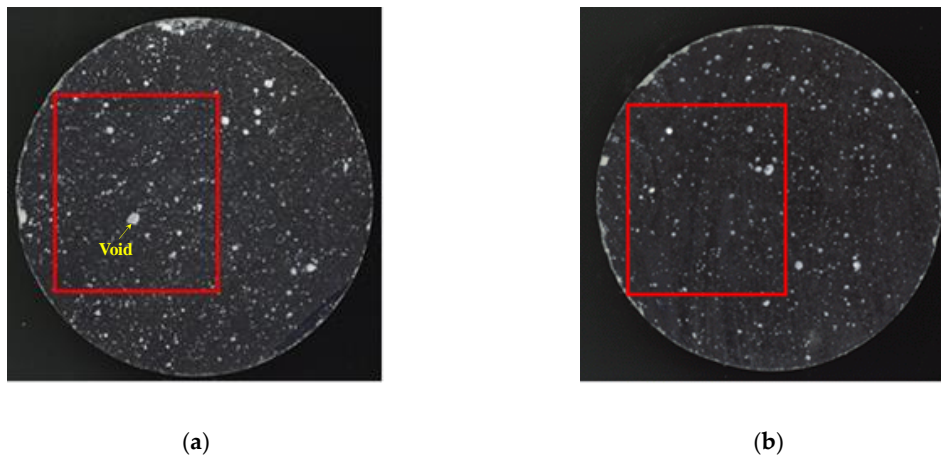


Figure 3. Evaluation of void distribution: (a) mortar; (b) matrix.

3. Pull-Out Test

In the present study, pull-out tests were conducted to evaluate the bond characteristics between the developed matrix and the textile, which composed the FRCM. The main parameters for pull-out test specimens were the type of textile that was used and the weaving type, as shown in Tables 5 and 6. Test specimens that contained carbon fibers were divided according to the type of coating into carbon-E (epoxy) and carbon-A (acrylate). Textile weaving methods are divided according to the type of textile that is used in glue bonding and thread bonding types. Test specimens were fabricated in accordance with ISO10406-1 methods [36]. Each specimen was composed of an embedded region, textile, and grip region, as shown in Figure 4a. The embedded region is the part that is embedded in the matrix. This part was fabricated using a cubic form (50 (Width) × 50 (Depth) × 20 (Height) mm). The embedded length of the matrix and textile was 20 (Length) mm. The total length of the textile was 200 mm, and the grip region was installed at the edge part of the textile using a steel plate. The grip size of the pull-out specimen was 50 (Height) × 25 (Width) mm.

Table 5. Mechanical properties of the textiles.

Textile Type	Area (mm ²)	Elastic Modulus (GPa)	Tensile Strength (GPa)	Ultimate Strain (%)
Carbon-E	1.810	220	3.3	1.5
Basalt-E	0.918	91	2.1	2.3
PET	2.560	8	1.0	12
Carbon-A	3.610	157	2.2	1.4
E-Glass	1.058	48	1.2	2.5

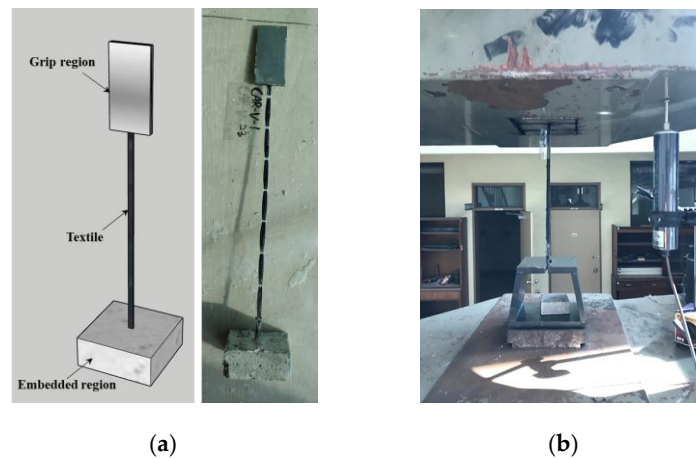


Figure 4. Test of pull-out series: (a) pull-out specimen; (b) setup of pull-out specimen.

As shown in Figure 4b, tests were performed using a UTM (Universal testing machine) with a capacity of 1000 kN, and an LVDT (Linear variable differential transducer) with a capacity of 200 mm was installed to measure the displacement of each pull-out specimen.

The pull-out test was carried out when the matrix reached 28 days, the loading speed for which was 0.01/min. In the present study, the pull-out bond strength between the matrix and textile was estimated using Equation (1) below:

$$\tau_{out} = \frac{P}{2L(w_f + t_f)} \tag{1}$$

Here, τ_{out} is the pull-out bond strength, P is the peak load, L is the embedment length of textile, w_f is the width of the textile, and t_f is the thickness of the textile.

3.1. Pull-Out Test Results

The final failure and bond stress–strain curves for the pull-out series for the matrix and textile are shown in Figures 5 and 6 and Table 6. Test results for all tested specimens are indicated as average values. The final failure occurred in the embedded region as the pull-out failure of the textile, as shown in Figure 5. As shown in Figure 6a, the pull-out bond strengths of the carbon textile type and basalt textile type were 3.19 and 1.87 MPa on average, respectively. With respect to the textile weaving type, the pull-out bond strength was highest in the basalt textile type at 1.87 MPa on average and lowest in the PET textile type at 1.23 MPa, as shown in Figure 6b.

Table 6. Properties of pull-out specimens and test results.

Various	Textile	Embedded Length	Coating	Configuration	Area (mm ²)	Peak Load (N)	Peak Stress (MPa)	Es (MPa)	Failure Mode *
Textile type	Carbon-E	20 mm	Epoxy		140	881	3.19	510	B
	Basalt				100	375	1.87	301	B
Weaving	PET		PVC		152	363	1.23	62	B
	Carbon-A		Acrylate		111	406	1.81	803	B
	Basalt		Epoxy		100	375	1.87	301	B
	E-Glass		Urethane		79	359	1.81	309	B

Note: * B: Pull-out failure; Amount of yarn: Carbon-E = 48 K; Basalt = 2400 deniers; PET = 24,000 deniers; Carbon-A = 50 K; E-Glass = 2400 TEX.

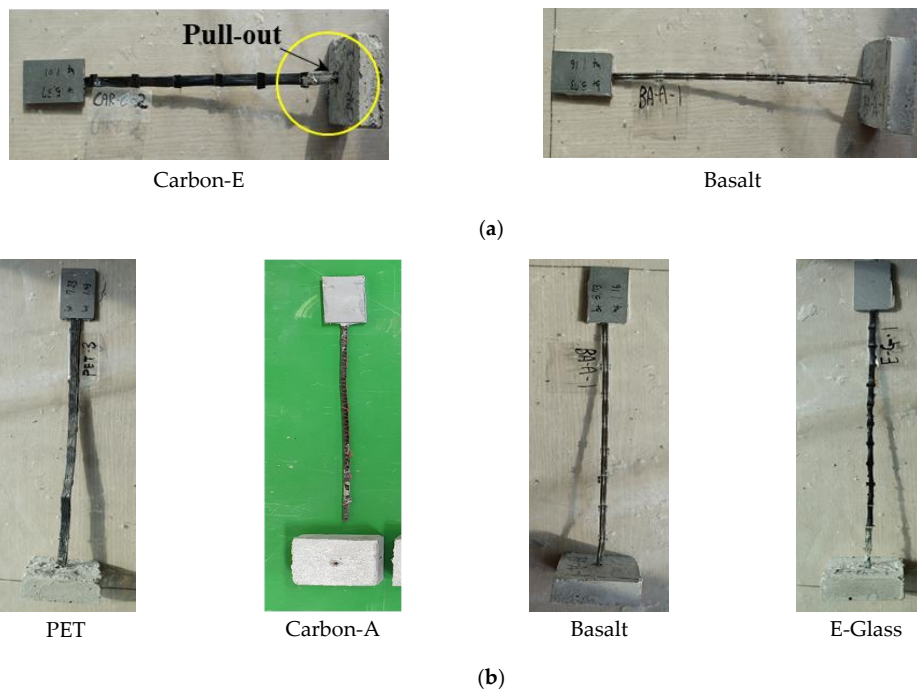


Figure 5. Failure in the pull-out series: (a) textile-type failure; (b) weaving-type failure.

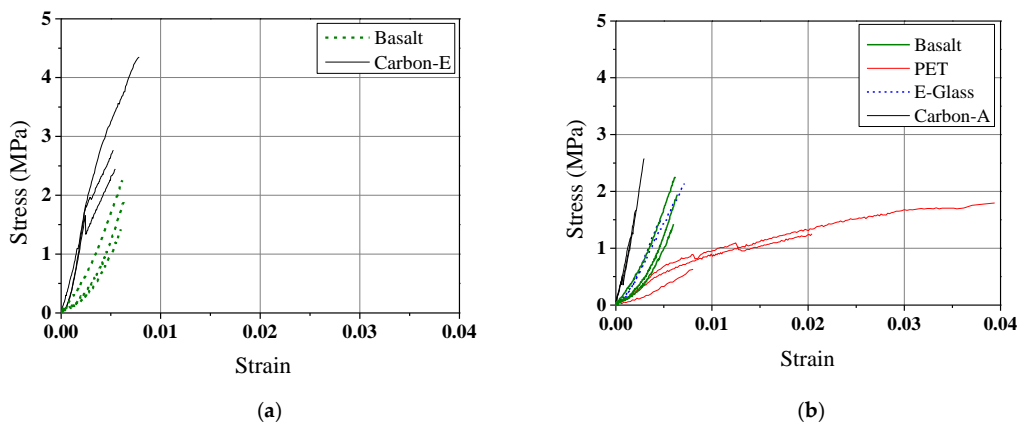


Figure 6. Stress–strain relationships of specimens: (a) type of textile; (b) type of weaving.

3.2. Pull-Off Test

In this study, a pull-off test was performed to evaluate the pull-off bond (direct bond) performance at the interface between the inorganic matrix and the textile grid. The main test parameters for pull-off test specimens were the type of textile used and the weaving methods. Test specimens were fabricated in accordance with ASTM C1583 [37], as shown in Figure 7. Each pull-off specimen was composed of a bottom plate ((70 (Width) × 70 (Depth) × 20 (Height) mm) made of the developed matrix and an upper grip (40 (Width) × 40 (Depth) × 10 (Height) mm), as shown in Figure 7a. As can be seen in Figure 7b, the textile was placed in the matrix between the bottom plate and the upper grip. The upper part of each pull-off specimen was attached with a loading grip using the epoxy bond. As shown in Figure 7d, the load was performed by connecting a loading device to a hydraulic jack with a capacity of 100 kN.

In the present study, the pull-off bond strength at the matrix–textile interface was estimated using Equation (2) below:

$$\tau_{off} = \frac{P}{A_e} \tag{2}$$

Here, τ_{off} is the pull-off bond strength, P is the peak load, and A_e is the area of the upper grip (40 (Width) \times 40 (Depth) = 1600 mm²).

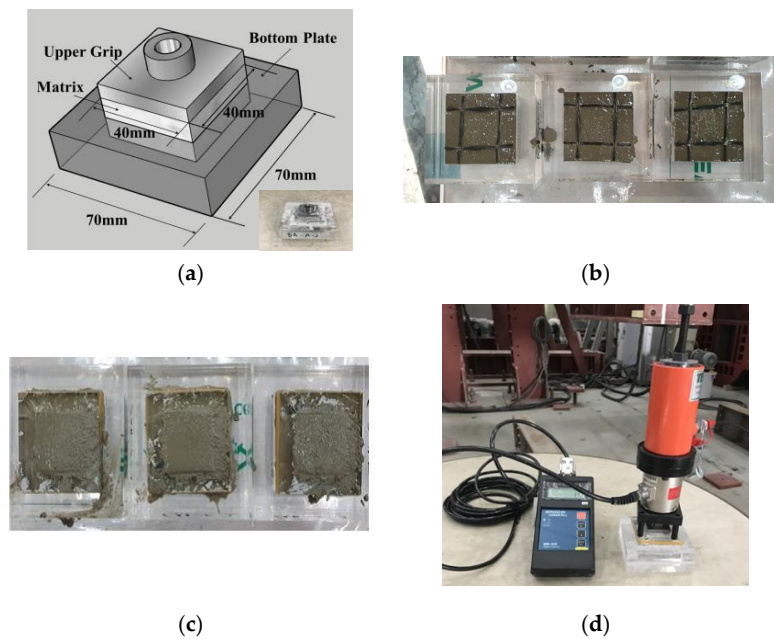


Figure 7. Test of pull-off series: (a) pull-off specimen; (b) arrangement of textiles; (c) pull-off specimens (after casting); (d) setup of pull-off specimen.

3.3. Pull-off Test Results

Table 7 and Figure 8 show the test results and final failure patterns of pull-off specimens. In all specimens, the matrix and textile between the upper grip and the bottom plate were subject to pull-off bond failure. When the textile type was considered, the pull-off bond strength was highest in the basalt textile type at 1.44 MPa. When the weaving type was considered, the pull-off bond strength was highest in the carbon textile type at 2.35 MPa.

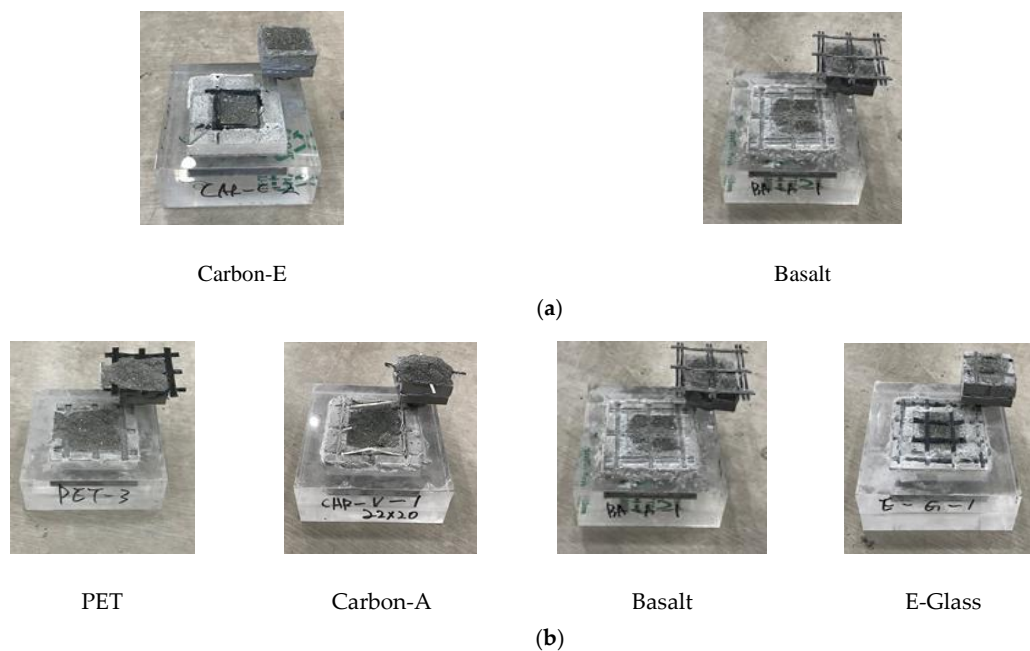


Figure 8. Failure of pull-out series: (a) textile-type failure; (b) weaving-type failure.

Table 7. Properties of pull-off specimens and test results.

Various	Textile	Grid Size (mm)	Coating	Configuration	Area (mm ²)	Peak Load (kN)	Peak Stress (MPa)	Failure Mode *
Textile type	Carbon-E	25 × 25	Epoxy		1600	2107	1.32	A
	Basalt					2303	1.44	A
Weaving	PET	25 × 25	PVC			3561	2.23	A
	Carbon-A	22 × 20	Acrylate			3757	2.35	A
	Basalt	25 × 25	Epoxy			2303	1.44	A
	E-Glass	20 × 20	Urethane			1323	0.83	A

* A: Failure at the matrix–textile interface.

4. Analysis

4.1. Pull-Out Test Results

In the present study, the elastic modulus at the maximum bond stress was determined based on the strain of the pull-out test specimens with respect to the bond stress. The elastic modulus of the pull-out test specimens is significant because it affects the bond strength between the matrix and textiles. As can be seen in Figure 9a, both the bond strength and elastic modulus were about 169% higher in the carbon-E type than in the basalt type. These results confirmed that the carbon-E textile allowed for excellent pull-out bond performance while being embedded in the developed matrix. When the textile weaving type was considered, all pull-out test specimens exhibited a comparable bond strength ranging between 1.23 and 1.87, as shown in Figure 9b. However, it was confirmed that the elastic modulus of the carbon-A type was 160–1300% higher than the other textile types. These results demonstrated that the carbon-A textile allowed for excellent initial bond stiffness while being embedded in the developed matrix.

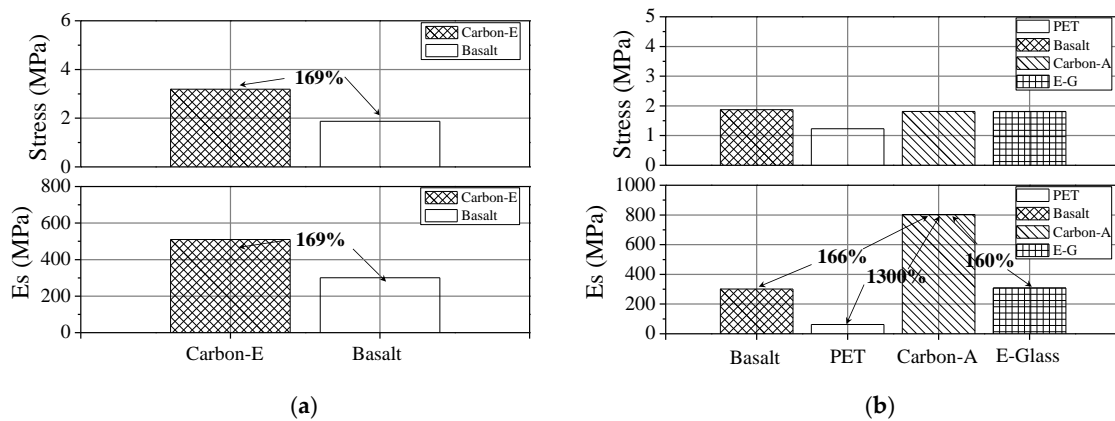


Figure 9. Analysis of pull-out specimens: (a) type of textile; (b) type of weaving.

4.2. Pull-Out and Pull-Off Bond Characteristics

The higher the pull-out and pull-off bond strengths are, the better the structural performance of the FRCM. Thus, in the present study, measured bond stress was compared according to the test method. As shown in Figure 10a, when the textile type was considered, the bond strength of the carbon-E textile type varied by up to 240% depending on the test method. However, the pull-off bond strength of the carbon-E textile and basalt textile types was comparable. Therefore, it was confirmed that the carbon-E textile allowed for excellent bond performance when combined with the developed matrix. When the textile weaving type was considered, the bond strength of the carbon-A textile type varied up to about 30% depending on the test method, but its pull-out and pull-off bond strengths were excellent compared to the other textile types. These results demonstrated that the carbon-E textile allowed for excellent bond performance when combined with the developed matrix.

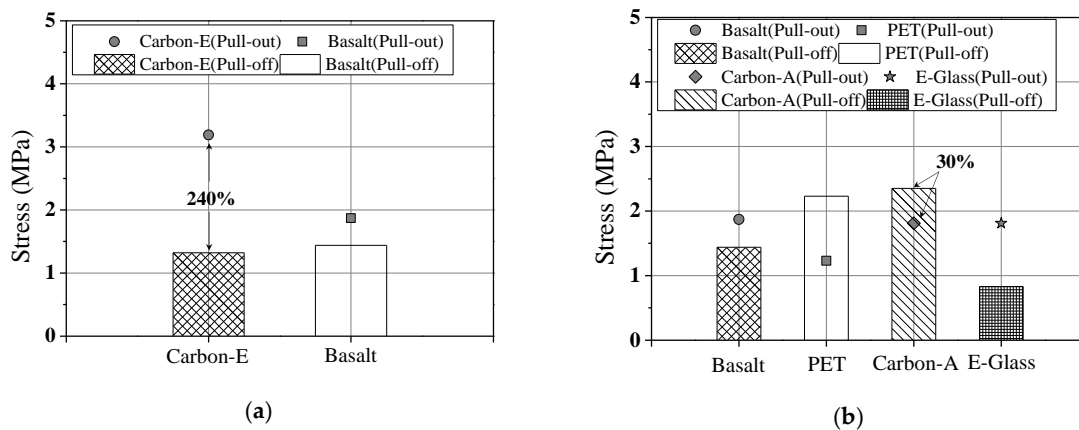


Figure 10. Comparison of bond stress with respect to the test method: (a) type of textile; (b) type of weaving.

5. Conclusions

In the present study, an inorganic cement adhesive incorporated in FRCM for use in the repair and reinforcement of RC structures was developed. Pull-out and pull-off tests were conducted to evaluate the bond characteristics in an attempt to assess its serviceability with textiles. The test results of this study were as follows.

The matrix developed through this study contained added single fibers, furnace slag, and silica fume, improving the physical properties and durability compared to existing mortar.

Pull-out test results showed that regardless of the type of coating agent or weaving method that were employed, the carbon textile allowed for the highest bond strength and elastic modulus while being embedded in the matrix. Meanwhile, pull-off test results also showed that the carbon textile allowed for excellent bond performance, similar to that shown in the pull-out test results.

Overall, these results demonstrated that carbon textiles were deemed to improve the repair and reinforcement performance of the FRCM when embedded in the matrix developed in this study. Future study is needed to evaluate the structural performance of RC members that contain FRCM, and thus assess its serviceability.

Author Contributions: Conceptualization, M.-J.K. and K.-H.K.; methodology, M.-J.K.; validation, H.-G.K. and M.-J.K.; formal analysis, Y.-J.L. and M.-S.J.; investigation, D.-H.K.; data curation, H.-G.K. and M.-J.K.; writing—original draft preparation, M.-J.K.; writing—review and editing, H.-G.K., M.-J.K., M.-S.J. and K.-H.K.; supervision, K.-H.K.; project administration, K.-H.K. All authors have read and agreed to the published version of the manuscript.

Funding: This research was supported by a grant (20CTAP-C152175-02) from Technology Advancement Research Program (TARP) funded by the Ministry of Land, Infrastructure, and Transport of the Korean government.

Conflicts of Interest: The authors declare no conflict of interest.

References

- Barnes, R.A.; Baglin, P.S.; Mays, G.C.; Subedi, N.K. External steel plate systems for the shear strengthening of reinforced concrete beams. *Eng. Struct.* **2001**, *23*, 1162–1176. [[CrossRef](#)]
- Aykac, S.; Kalkan, I.; Aykac, B.; Karahan, S.; Kayar, S. Strengthening and repair of reinforced concrete beams using external steel plates. *J. Struct. Eng.* **2012**, *139*, 929–939. [[CrossRef](#)]
- Chang, C.H.; Kwon, M.H.; Kim, J.S.; Joo, C.H. Numerical study for seismic strengthening of RC columns using fiber reinforced plastic composite. *J. Korea Inst. Struct. Maint. Insp.* **2012**, *16*, 117–127. (In Korean)
- Mander, J.; Priestley, M.; Park, R. Theoretical stress-strain model for confined concrete. *J. Struct. Eng.* **1988**, *114*, 1804–1826. [[CrossRef](#)]
- Kim, J.S.; Seo, H.S.; Lim, J.H.; Kwon, M.H. An performance evaluation of seismic retrofitted column using FRP composite reinforcement for rapid retrofitting. *J. Korea Concr. Inst.* **2014**, *26*, 47–55. (In Korean) [[CrossRef](#)]

6. Kim, M.J.; Kim, H.G.; Lee, J.Y.; Jo, M.S.; Kim, K.H. Evaluation of flexural performance of RC columns reinforced with hybrid FRP sheets. *J. Korea Concr. Inst.* **2019**, *31*, 611–618. (In Korean) [[CrossRef](#)]
7. Ha, S.S.; Choi, D.U.; Lee, J.Y.; Kim, K.H. Pseudo-ductile hybrid FRP sheet for strengthening reinforced concrete beams. *J. Korea Concr. Inst.* **2008**, *20*, 239–247. (In Korean)
8. Choi, D.U.; Kang, T.H.K.; Ha, S.S.; Kim, K.H.; Kim, W.S. Flexural and bond behavior of concrete beams strengthened with hybrid carbon-glass fiber-reinforced polymer sheets. *ACI Struct. J.* **2011**, *108*, 90–98.
9. Awani, O.; El-Maaddawy, T.; Ismail, N. Fabric-reinforced cementitious matrix: A promising strengthening technique for concrete structures. *Constr. Build. Mater.* **2017**, *132*, 94–111. [[CrossRef](#)]
10. Stang, H. Significance of shrinkage-induced clamping pressure in fiber-matrix bonding in cementitious composite materials. *Adv. Cem. Based Mater.* **1996**, *4*, 106–115. [[CrossRef](#)]
11. Hempel, S.; Butler, M.; Mechtcherine, V. Bond behaviour and durability of basalt fibers in cementitious matrices. In *3rd ICTR International Conference on Textile Reinforced Concrete*; Bramshuber, W., Ed.; Rilem publications sarl: Aachen, Germany, 2015.
12. Butler, M.; Mechtcherine, V.; Hempel, S. Experimental investigations on the durability of fibre-matrix interfaces in textile-reinforced concrete. *Cem. Concr. Compos.* **2009**, *31*, 221–231.
13. Abdel-Magid, B.; Ziaee, S.; Gass, K.; Schneider, M. The combined effects of load, moisture and temperature on the properties of E-glass/epoxy composites. *Comp Struct.* **2005**, *71*, 320–326. [[CrossRef](#)]
14. Peled, A.; Bentur, A. Geometrical characteristics and efficiency of textile fabrics for reinforcing composites. *Cem. Concr. Res.* **2000**, *30*, 781–790. [[CrossRef](#)]
15. Peled, A.; Bentur, A. Fabric structure and its reinforcing efficiency in textile reinforced cement composites. *Compos. A* **2003**, *34*, 107–118.
16. ACI Committee 549. *Guide to Design and Construction of Externally Bonded Fabric-Reinforced Cementitious Matrix (FRCM) Systems for Repair and Strengthening Concrete and Masonry Structures (ACI 549.4R-13)*; American Concrete Institute: Farmington Hills, MI, USA, 2013.
17. Ortlepp, R.; Hampel, U.; Curbach, M. A new approach for evaluating bond capacity of TRC strengthening. *Cem. Concr. Compos.* **2006**, *28*, 589–597.
18. Hashemi, S.; Al-Mahaidi, R. Investigation of bond strength and flexural behaviour of FRP-strengthened reinforced concrete beams using cement based adhesives. *J. Struct. Eng.* **2010**, *11*, 129–139.
19. D’Ambrisi, A.; Feo, L.; Focacci, F. Experimental analysis on bond between PBO FRCM strengthening materials and concrete. *Compos. B* **2013**, *44*, 524–532.
20. Sneed, L.H.; D’Antino, T.; Carloni, C. Investigation of bond behavior of polyparaphenylene benzobisoxazole fiber-reinforced cementitious matrix composite-concrete interface. *ACI Mater. J.* **2014**, *111*, 569–580.
21. Awani, O.; El Refai, A.; El-Maaddawy, T. Bond characteristics of carbon fabric reinforced cementitious matrix in double shear tests. *Constr. Build. Mater.* **2015**, *101*, 39–49. [[CrossRef](#)]
22. D’Antino, T.; Carloni, C.; Sneed, L.H.; Pellegrino, C. Fatigue and post-fatigue behavior of PBO FRCM-concrete joints. *Int. J. Fatigue* **2015**, *81*, 91–104. [[CrossRef](#)]
23. Ombres, L. Analysis of the bond between fabric reinforced cementitious mortar (FRCM) strengthening systems and concrete. *Compos. B* **2015**, *69*, 418–426. [[CrossRef](#)]
24. Sneed, L.H.; D’Antino, T.; Carloni, C.; Pellegrino, C. A comparison of the bond behavior of PBO-FRCM composites determined by double-lap and single-lap shear tests. *Cem. Concr. Compos.* **2015**, *64*, 37–48.
25. D’Antino, T.; Sneed, L.H.; Carloni, C.; Pellegrino, C. Effect of the inherent eccentricity in single-lap direct-shear tests of PBO FRCM-concrete joints. *Compos. Struct.* **2016**, *142*, 117–129.
26. Ombres, L.; Iorfida, A.; Mazzuca, S.; Verre, S. Bond analysis of thermally conditioned FRCM-masonry joints. *Measurement* **2018**, *125*, 509–515.
27. Colombo, I.G.; Magri, A.; Zani, G.; Colombo, M.; Di Prisco, M. Erratum: Textile reinforced concrete: Experimental investigation on design parameters. *Mater. Struct.* **2013**, *46*, 1953–1971. [[CrossRef](#)]
28. Portal, W.N.; Flansbjer, M.; Johannesson, P.; Malaga, K.; Lundgren, K. Tensile behaviour of textile reinforcement under accelerated aging conditions. *J. Build. Eng.* **2016**, *5*, 57–66. [[CrossRef](#)]
29. De Munck, M.; El Kadi, M.; Tsangouri, E.; Vervloet, J.; Verbruggen, S.; Wastiels, J.; Tysmans, T.; Remy, O. Influence of environmental loading on the tensile and cracking behaviour of textile reinforced cementitious composites. *Constr. Build. Mater.* **2018**, *181*, 325–334.

30. Iorfida, A.; Verre, S.; Candamano, S.; Ombres, L. Tensile and direct shear responses of baslat-fibre reinforced mortar based materials. In Proceedings of the Strain-Hardening Cement-Based Composites (SHCC4), Deresden, Germany, 18–20 September 2017; RILEM: Aachen, Germany, 2018; pp. 544–552.
31. Bencardino, F.; Nisticò, M.; Verre, S. Experimental investigation and numerical analysis of bond behavior in SRG-strengthened masonry prisms using UHTSS and stainless-steel fibers. *Fibers* **2020**, *8*, 8.
32. ISO. Cement—Test Methods—Determination of Strength. ISO 679. 2009. Available online: <https://www.iso.org/standard/45568.html> (accessed on 1 October 2018).
33. Korea Standards F 4042. *Polymer Modified Cement Mortar for Maintenance in Concrete Structure*; Korean Agency for Technology and Standard: Seoul, Korea, 2017.
34. ASTM C1403-15. *Standard Test Method for Rate of Water Absorption of Masonry Mortars*; ASTM: West Conshohocken, PA, USA, 2015.
35. ASTM C 457. *Standard Practice for Microscopical Determination of Air Void Content and Parameters of the Air Void System in Hardened Concrete*; ASTM: West Conshohocken, PA, USA, 2004.
36. International Organization for Standardization (ISO). *ISO 10406-1 Fibre-Reinforced Polymer (FRP) Reinforcement of Concrete: Test Methods: Part 1: FRP Bars and Grid*; ISO: Geneva, Switzerland, 2015.
37. ASTM C1583/C1583M-13. *Standard Test Method for Tensile Strength of Concrete Surfaces and the Bond Strength or Tensile Strength of Concrete Repair or Overlay Materials by Direct Tension (Pull-Off Method)*; ASTM: West Conshohocken, PA, USA, 2013.



© 2020 by the authors. Licensee MDPI, Basel, Switzerland. This article is an open access article distributed under the terms and conditions of the Creative Commons Attribution (CC BY) license (<http://creativecommons.org/licenses/by/4.0/>).